A Structural Model of the Tetrodotoxin and Saxitoxin Binding Site of the Na^+ Channel

Gregory M. Lipkind and Harry A. Fozzard

The Cardiac Electrophysiology Laboratories, and The Departments of Pharmacological and Physiological Sciences, Biochemistry and Molecular Biology and Medicine, The University of Chicago, Chicago, Illinois 60637 USA

ABSTRACT Biophysical evidence has placed the binding site for the naturally occurring marine toxins tetrodotoxin (TTX) and saxitoxin (STX) in the external mouth of the Na^+ channel ion permeation pathway. We developed a molecular model of the binding pocket for TTX and STX, composed of antiparallel β-hairpins formed from peptide segments of the four S5–S6 loops of the voltage-gated Na^+ channel. For TTX the guanidinium moiety formed salt bridges with three carboxyls, while two toxin hydroxyls (C9-OH and C10-OH) interacted with a fourth carboxyl on repeats I and II. This alignment also resulted in a hydrophobic interaction with an aromatic ring of phenylalanine or tyrosine residues for the brainII and skeletal Na^+ channel isoforms, but not with the cysteine found in the cardiac isoform. In comparison to TTX, there was an additional interaction site for STX through its second guanidinium group with a carboxyl on repeat IV. This model satisfactorily reproduced the effects of mutations in the S5–S6 regions and the differences in affinity by various toxin analogs. However, this model differed in important ways from previously published models for the outer vestibule and the selectivity region of the Na^+ channel pore. Removal of the toxins from the pocket formed by the four β-hairpins revealed a structure resembling a funnel that terminated in a narrowed region suitable as a candidate for the selectivity filter of the channel. This region contained two carboxyls (Asp^{384} and Glu^{942}) that substituted for molecules of water from the hydrated Na^+ ion. Simulation of mutations in this region that have produced Ca^{2+} permeation of the Na^+ channel created a site with three carboxyls (Asp^{384}, Glu^{942}, and Glu^{1714}) in proximity.

INTRODUCTION

Tetrodotoxin (TTX) and saxitoxin (STX) are naturally occurring high affinity marine toxins that selectively block the voltage-sensitive Na^+ channel (Hille, 1992; Catterall, 1992). Their overlapping binding sites are most probably located in the outside mouth of the ion permeation pathway. Although the chemical structures of TTX and STX (see Fig. 1) are quite different, their biological activities are virtually identical, partly as a consequence of a shared guanidinium group that is positively charged at physiological pH. One or more negatively charged carboxyl groups on the channel protein have been shown to play an essential role in toxin binding by either pH titration or by treatment with carboxyl-modifying reagents (Hille, 1968; Shrager and Profera, 1973). The guanidinium ion itself is permeant to the Na^+ channel (Hille, 1971), and both permeant and non-permeant (blocking) cations can compete for the toxin site (Narahashi, 1974). On the basis of such data, Hille (1975) suggested that the guanidinium group of TTX is bound to a rectangular ring of six oxygens located in the walls of the channel pore at its selectivity filter, with the cationic guanidinium forming a salt bridge to one negatively charged acid group and with other polar groups of the toxin interacting with the remaining oxygens so as to occlude the pore.

In 1984 Numa and coworkers (Noda et al., 1984) cloned the first of a family of isoforms of the principal subunit of the Na^+ channel. These Na^+ channel α-subunits are large glycoproteins of about 2000 amino acids, organized into four highly homologous domains or repeats (I–IV). Each domain includes six transmembrane segments (S1–S6) with high α-helical potential (Numa and Noda, 1986). On the basis of biophysical and chemical data the extracellular segment between S5 and S6 of each repeat is thought to fold back into the membrane to form part of the ion-conducting pathway (Guy and Conti, 1990). A series of point mutations in this S5–S6 segment by Stühmer, Numa, and colleagues and others (Noda et al., 1989; Terlau et al., 1991; Satin et al., 1992; Backx et al., 1992; Heinemann et al., 1992a; Kontis and Goldin, 1993) has identified several specific amino acids essential for toxin block and for isoform differences in toxin affinity.

The size and solubility characteristics of the Na^+ channel preclude determination of the three-dimensional structure of this large molecule at this time. However, the primary structures of several isoforms are known, along with effects of point mutations that affect toxin binding. We used this information to develop a model of the toxin binding pocket from parts of the S5–S6 loops that have been identified as probable parts of the outer vestibule of the channel pore. The model was based on the simple question if a reasonable structural organization of the amino acids in this region could be arranged around the toxin molecules so as to form an interaction that satisfied the available analog and mutation data. Working with only a small fraction of the entire protein sequence, we found a predicted structure of these short peptide

Received for publication 22 July 1993 and in final form 12 October 1993.

Address reprint requests to Dr. Harry A. Fozzard at MC 6094, 5841 S. Maryland Ave., Chicago, IL 60637. Tel.: 312-702-1481; fax: 313-702-6789.

0006-3495/94/01/01/13 $2.00

segments that interacted well with the toxins, yielding a binding pocket conforming to the available experimental toxin analog and channel point mutation data and to channel isoform differences in toxin block.

EXPERIMENTAL RESULTS USED IN MODEL DEVELOPMENT

The construction and constraints of this model depend strongly on experimental studies of block by toxins and their analogs, and on the available data on point mutations in cloned Na^+ channels.

Blockade by various guanidinium toxins

Kao and coworkers (see review by Kao, 1986) have identified the active groups in TTX and STX. In the case of TTX these are the guanidinium group and the hydroxyls at C9 and C10 (see Fig. 1). The guanidinium group is thought to form an ion-pair with an anionic site of the receptor, while the C9-OH and C10-OH form hydrogen bonds with other sites (Kao and Walker, 1982). The latter suggestion was confirmed by the low (0.01–0.02 ×) affinity of the analog anhydrotetrodotoxin, where C4 and C9 are joined by an oxygen bridge (Narahashi et al., 1967; Kao and Yasumoto, 1985). 4-Epitetrodotoxin, in which the positions of the -H and -OH were reversed from TTX, is about 0.5 × as potent as TTX. Therefore, the change in activity of anhydrotetrodotoxin can be explained as loss of the C9-OH group and one of the hydrogen bonds to the binding site. Modifications of both C9-OH and C10-OH in the case of tetrodonic acid led to a totally ineffective molecule (Narahashi et al., 1967). 6-Epitetrodotoxin and 11-deoxytetrodotoxin have low binding affinity (about 0.01 ×) to Na^+ channels (Yang et al., 1992a). However, nortetrodotoxin and nortetrodotoxin alcohol, which cannot form corresponding hydrogen bonds, were somewhat less potent than TTX (Kao, 1982), implying that the C6 end of TTX is not very important for channel block.

In prior studies of STX, the 7,8,9-guanidinium group and two C12 hydroxyls were identified as important for STX binding (Strichartz, 1984; Kao, 1986). The two hydroxyls can be reduced selectively to produce either the α or the β epimer of saxitoxinol, which have blocking affinity of only 0.01 × (Koehn et al., 1981; Kao et al., 1985). Koehn et al. (1981) concluded that the carbamoyl group of STX (H_2NCO-group as substitute at C6) contributes to, but is not essential for channel blockade, because decarbamoylsaxitoxin (dcSTX) is about 0.2 × as active as STX. Besides, an acetyl derivative of dcSTX, in which an amino group was substituted by a methyl group, has shown the same activity (Mahar et al., 1991). Nevertheless, the potency of decarbamoyloxysaxitoxin is only 0.008 × that of STX (Yang et al., 1992b).

Yang and Kao (1992) identify seven possible interaction sites in the structures of TTX and STX that they conclude are important, but a more conservative analysis suggests that only the guanidinium group and the two hydroxyls at C9 and C10 (for TTX) or C12 (for STX) are the most critical sites. These sites show remarkable stereospecific similarities and appear to determine the high toxin specificity. When the guanidinium group of TTX and the 7,8,9-guanidinium group of STX are aligned, then the hydroxyls at C9 and C10 for TTX and the two hydroxyls at C12 for STX are also closely aligned (Kao and Walker, 1982). The positive charge in the second 1,2,3-guanidinium group of STX may also be involved, but direct evidence is lacking. Finally, chiriquitoxin (CqTX) differs from TTX only by a glycine residue in place of a hydrogen of the hydroxymethyl group at position C11, but at pH 7.25 it has equal block potency as TTX (Yang and Kao, 1992). Since glycine has high potency for formation of hydrogen bonds but its presence does not modify binding, the C11 site is most probably outside of the vestibule and not able to interact with the binding pocket.

Inference for binding from mutation studies

Site-directed mutations of the conserved amino acids of the rat brain II (rBrII), the adult skeletal, and the cardiac α-subunits of the Na^+ channel have provided important information about the amino acids residues required for TTX and STX binding. We are indebted to the extensive work of Stühmer, Numa, and colleagues for explorations of the amino acids previously suggested by Guy and Conti (1990) to be part of the pore and named SS1-SS2 or the P loop. A single point mutation of glutamic acid 387 (rBrII number) to glutamine (E387Q) results in complete loss of TTX and STX block (Noda et al., 1989). Glu^{387} belongs to the SS2 segment of repeat I (Fig. 2). Terlau et al. (1991) made systematic mutations in residues of the SS2 segments of repeats I–IV. Neutralization of any of the six conserved residues of Glu or Asp reduced the sensitivity to TTX and STX block by at least three orders of magnitude (Table 1). Charge mutations at other adjacent positions produced smaller changes in toxin block. Terlau et al. (1991) suggested that there are two clusters of negatively charged residues at equivalent positions in the SS2 segments of repeats I–IV (marked by *arrows* in Fig. 2). The most dramatic effect on toxin block in their study was produced by neutralization of the carboxyl residues on repeats I and II. Neutralization of aspartic acid at position 1717 of repeat IV (D1717N) abolished STX block, while partially

TABLE 1 Effects of single mutations on TTX and STX sensitivities and single channel conductance

Mutant	Repeat	IC_{50}, TTX	IC_{50}, STX	Conductance
		nM	nM	pS
Wild-type		18 ± 4	1.2 ± 0.2	15.4
D384N	I	>10000	>1000	<0.1
E387Q		>10000	>1000	3.1
E942Q	II	>10000	>1000	<0.5
E945Q		2800 ± 180	>1000	8.2
D1426N	III	30 ± 10	8.9 ± 0.4	14.0
D1717N	IV	350 ± 90	>1000	8.8

Data from Terlau et al. (1991).

reducing the block by TTX. In repeat III neutralization of Asp^{1426} (mutant D1426N) had little effect on either toxin. Finally, the cardiac isoform has a lower affinity for both toxins, which appears to be a consequence of the absence of an aromatic ring residue (Tyr or Phe) at position 385 in the rBrII number system (Satin et al., 1992; Backx et al., 1992; Heinemann et al., 1992a).

STRUCTURAL MOTIF FOR THE TTX/STX BINDING SITE

For this model we infer that a residue is involved in a nonbonding or electrostatic interaction with the toxin if its substitution changes the toxin blocking affinity 100–1000 ×. Effects on binding affinity less that 10 × can be physiologically interesting, but beyond the accuracy of the present model.

Scheme of principal sites of interaction

In agreement with the experimental results of Terlau et al. (1991), we assumed that similar structural elements of the two toxins interact with residues of repeats I and II (Table 1). The guanidinium group and the hydroxyls C9-OH and C10-OH of TTX and the 7,8,9-guanidinium group and the hydroxyls at C12 of STX interact primarily with carboxyls at positions 384, 387, 942, and 945. The 1,2,3-guanidinium group of STX may interact with the carboxyl at position 1717 of repeat IV, which has much less influence on TTX block (Table 1). We propose that three of the carboxyls of repeats I and II interact with the guanidinium group, while the fourth negatively charged residue forms two hydrogen bonds with neighboring hydroxyl groups of C9 and C10 for TTX and C12 for STX. Among the four carboxyl sites Glu^{945} appears to be less important for TTX binding than the others, since the mutation E945Q reduces TTX sensitivity less than the other mutations. Most probably, Glu^{945} interacts with the TTX hydroxyls. Indeed, the hydrogen bond formed by the C10-OH group is rather weak, as indicated by its easy deprotonization (Kao, 1986). On the other hand, both hydrogen bonds formed by the gem-diol group of STX are strong, so that Glu^{945} is as important as the other carboxyls for STX binding (Kontis and Goldin, 1993). It seems plausible that Glu^{945} interacts with the toxin hydroxyls, and the other three carboxyls at positions 384, 387, and 942 form ion-pair salt bridges with the guanidinium group.

We will consider an arrangement for toxin binding that includes four loci for TTX and five loci for STX (Fig. 1). This scheme is in accordance with the three resonance forms of the guanidinium, in which the positive charge is distributed between the N—H groups. Moreover, there are examples in proteins where different N—H groups of Arg form salt bridges with some carboxyl groups of Asp or Glu (Proegman et al., 1978). Consequently, each of the three carboxyl residues would contribute almost equally to interaction with the guanidinium group, and the fourth carboxyl group gives approximately similar energetic contribution. Fersht et al. (1985) showed that the energy of a salt bridge is approximately equal to that of two neutral hydrogen bonds.

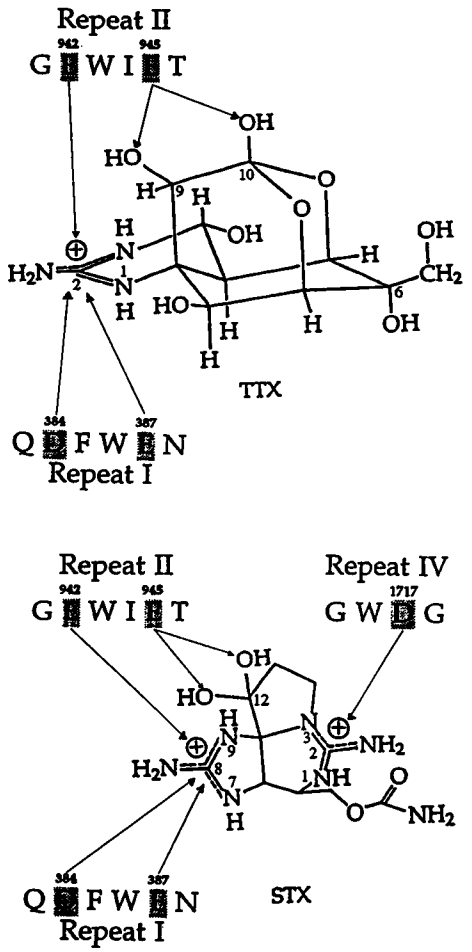

FIGURE 1 Molecular structures of TTX and STX and suggested amino acid interactions of the Na^+ channel (see Fig. 2). There are four loci for TTX and five loci for STX. The toxin structures are from Hille (1992).

Conformation of the SS1 and SS2 peptide fragments

The first step in predicting a satisfactory protein structure for toxin interaction was to examine the probable structural properties of the peptide chains comprising the SS1 and SS2 segments from the four repeats of rBrII (Fig. 2), taking into

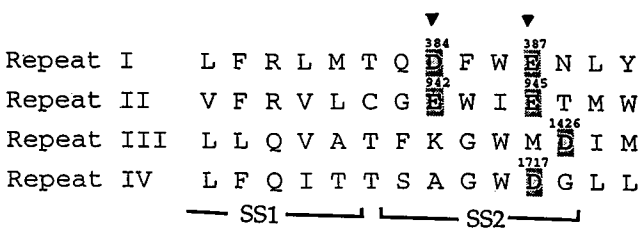

FIGURE 2 The SS1-SS2 regions (P-loops) of repeats I–IV of the rat brain II Na^+ channel. Positions of certain critical mutations are marked (from Terlau et al. (1991)).

account the probably extracellular location of these segments. SS1 and SS2 contain many residues that have high probability for appearance in β-strands or β-structures: Val, Ile, Tyr, Cys, Trp, Phe, Thr, Met, and Leu (Creighton, 1993). For example, in the case of the SS1 fragment of repeat II there are five bulky hydrophobic residues in the C-terminal six-member segment: Ile, Val, Leu, and Phe (Fig. 2). On the other hand, residues at the border between SS1 and SS2 have a conformational preference to participate in reverse β-turns: Gly, Asp, Ser, and Lys (Wilmot and Thornton, 1988). Therefore, this region has a high probability to form β-hairpins, in which adjacent β-strands are linked through β-turns and produce a structure that might exist at an interface between the hydrophilic surface and the hydrophobic core or the protein.

In order to select likely positions for the β-turns in the peptide chains we used the procedure proposed by Chou and Fasman (1978), but taking into account newer values for the conformational preferences (P_t) found on the basis of x-ray data of proteins (Williams et al., 1987). The values of P_t characterize the relative tendencies of residues to be involved in β-turns (Table 2). Values of $P_t > 1.0$ characterize amino acid residues favoring β-turns. According to Chou and Fasman (1978), a β-turn is predicted if a four-residue sequence has an average value $\langle P_t \rangle > 1$ (and $\langle P_t \rangle > \langle P_\beta \rangle$). Further, values of P_t for the two central residues of the β-turn should be greater than those for the extreme residues. These conditions are reasonably met on the central portions of the four peptide fragments underlined in Table 2 ($\langle P_t \rangle$ = 0.96, 0.99, 1.02, and 1.12, respectively). The sequences preceding the proposed β-turns are composed of residues with low probability of participating in turns. For repeat IV a second possible turn region is seen, but we selected the first one for reasons presented later. In this manner, we chose the four β-hairpins of repeats I–IV, composed of two β-strands connected in the center by β-turns (as marked in Table 2), and consisting of 10 residues each. It was important to include all of the SS2 amino acids, in order to stabilize the β-hairpin. The 1–2 adjacent residues on both ends also have a high probability of being in β-strands, and the usual length of such β-hairpins is 8–16 amino acids (Sibanda et al., 1989). Since these are no longer identical with the original definition of the SS1 and SS2 segments, we will call them beta1 and beta2 on the N and C ends, respectively.

The conformations of the β-hairpins are important for our modelled structure, because they determine the characteristic orientation of side chains (Fig. 3). We adopted the usual numbering for the four residues that comprise β-turns (i, i + 1, i + 2, and i + 3) (Creighton, 1993). Neighboring residues of the β-strands alternate relative to the plane of the β-hairpin (up-down-up...). Residues i and i + 3 belong to both the β-turn and the β-strand. If residues i + 2, i + 3, and i + 5 of beta2 are located on the outside plane of the β-hairpin, the residues i + 1, i + 4, and i + 6 are found on the opposite side. In repeat I we know from mutation studies that Asp^{384} (i + 2) is important for toxin block. Therefore, Phe^{385} (i + 3), and Glu^{387} (i + 5) would be important for toxin block, also consistent with mutation data, and other residues of the fragment that face away from the toxin site would be relatively unimportant. In like manner we can predict for repeat II that only residues in positions i + 2, i + 3, and i + 5 (Glu^{942}, Trp^{943}, and Glu^{945}) have the correct location to interact with toxin. Effects of these residues would be large (two to four orders of magnitude), while other residues would produce only small effects on toxin interaction by secondary changes in the binding structure.

TTX interacted with primarily the segments of repeats I and II. These two repeats can be aligned to form a structure consisting of two antiparallel β-hairpins adjacent to each other. This structure produces a cavity for binding of TTX, with the inner part consisting of six side chains of residues Asp^{384}, Phe^{385}, Glu^{387}, Glu^{942}, Trp^{943}, and Glu^{945} (Fig. 4). Presumably the β-hairpins of repeats III and IV form mainly the outer walls of the binding cavity for TTX, with the β-hairpins also arranged in an antiparallel fashion. For repeat III this results in the possibility of toxin interaction with the residues of Lys^{1422} (i + 1), Met^{1425} (i + 4), and Ile^{1427} (i + 6). The residues of interest for repeat IV in the arrangement are Ala^{1714} (i + 1), Asp^{1717} (i + 4), and Leu^{1719} (i + 6). Indeed, alignment of the β-hairpin of repeat IV in an antiparallel relationship to that of repeat I on the front wall changes the directions of its side chains in space, so that the side chains of residues i + 1, i + 4, and i + 6 are inside the

TABLE 2 Conformational preferences P_t* for residues in SS1–SS2 segments of the muscle channel and positions of β-turns (*underlined*)

								384			387		
Repeat I	L	F	R	L	M	T	Q	D	Y	W	E	N	L
P_t	0.57	0.59	0.90	0.57	0.52	0.90	0.84	1.24	0.86	0.65	1.01	1.34	0.57
								942			945		
Repeat II	V	F	R	V	L	C	G	E	W	I	E	T	M
P_t	0.41	0.59	0.90	0.41	0.57	0.54	1.77	1.01	0.65	0.47	1.01	0.90	0.52
								1422			1425		
Repeat III	L	L	Q	V	A	T	F	K	G	W	M	D	I
P_t	0.57	0.57	0.84	0.41	0.82	0.90	0.59	1.07	1.77	0.65	0.52	1.24	0.47
								1714			1717		
Repeat IV	L	F	Q	I	T	T	S	A	G	W	D	G	L
P_t	0.57	0.59	0.84	0.47	0.90	0.90	1.22	0.82	1.77	0.65	1.24	1.77	0.57

* From Williams et al. (1987).

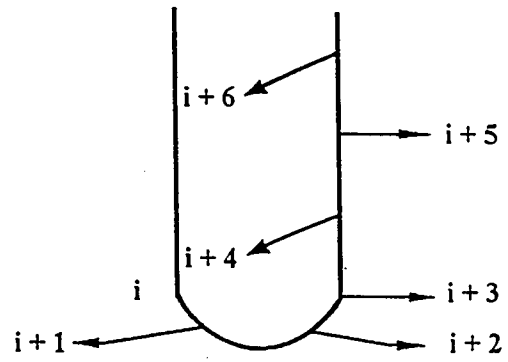

FIGURE 3 Directions of side chains in the β-hairpins. The residues in the β-turns are numbered i to $i + 3$.

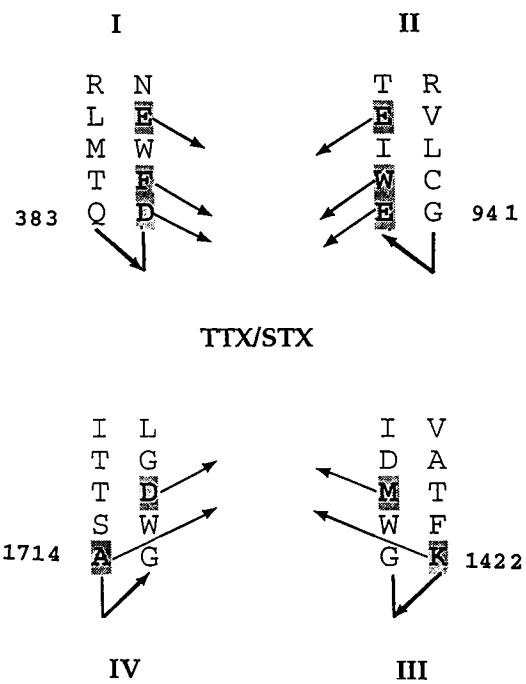

FIGURE 4 Structural motif for the TTX/STX binding site of the Na^+ channel—an antiparallel arrangement of β-hairpins of repeats I–IV. Residues that interact with toxins are marked by arrows. The numbered residues are located in positions $i + 1$ of β-turns. Relative orientation of β-turns of the four hairpins is shown by flat arrows connecting the beta1 and beta2 strands, and it corresponds to an overhead view.

binding cavity. In this model the residues at $i + 6$ can be ignored, because they are above the level of the toxin molecule. This structural motif of the toxin binding site forms a funnel-like aggregate barrel, consisting of four antiparallel β-hairpins with the beta2 strands facing the vestibule and the beta1 strands on the outside toward the protein core (Fig. 4).

Comparison of the structural motif to mutation data

The arrangement of the four β-hairpins into an antiparallel structure results in a vestibule-like cavity appropriately sized for a toxin binding pocket. Although some of the mutation data were used to make our initial selection of interactive sites, model predicts correctly the results of mutation of all of the residues reported by Terlau et al. (1991). Neutralization of the aspartic and glutamic acid residues (but not swapping these residues) at positions $i + 2$ and $i + 5$ of repeat I and $i + 2$ of repeat II resulted in loss of both TTX and STX block (Table 1). Neutralization of glutamic acid at position $i + 5$ of repeat II greatly reduces toxin block, similar to the effect of toxin analogs that affect the hydroxyl sites. The model also predicts possible participation of the residue at positions $i + 3$ in repeat I. Satin et al. (1992) demonstrated that substitution of Phe^{385} or Tyr in place of the naturally occurring Cys resulted in an increase in TTX and STX affinity of about 1000 ×. Backx et al. (1992) found that the reverse mutation of tyrosine to cysteine in the skeletal isoform reduced toxin affinity dramatically, and Heinemann et al. (1992a) demonstrated the same effect for mutation of phenylalanine to cysteine in rBrII. Terlau et al. (1991) reported mutations in repeats I and II in positions $i + 1$ (Q383E, Q383K, G941E) and $i + 6$ (N388R) that had less than 10-fold effects on toxin block. The W386C mutation at $i + 4$, which reduced TTX block 30-fold (Tomaselli et al., 1993), is a very nonconservative change, and it undoubtedly caused some structural reorganization of the vestibule. Mutations beyond the 10 amino acid β-hairpins modelled here (R379Q, Q391K, D949N, E952Q) had little effect (Terlau et al., 1991; Kontis and Goldin, 1993), suggesting that the dimensions of the proposed vestibule are appropriate.

The mutants of residue Asp^{1426} in repeat III and of residue Asp^{1717} in repeat IV represent a good test of the antiparallel alignment of the β-hairpins. This model predicts that side chains in position $i + 5$ of repeats III and IV are directed outside the pocket. Indeed, mutants of this carboxyl of repeat III (D1426N, D1426Q, D1426K) do not affect toxin block significantly (Table 1). On the other hand, substitution by a positive charge at position $i + 4$ of repeat III did interfere with block of both toxins (M1425K). In repeat IV position $i + 4$ is active, and all three mutants of Asp^{1717}—D1717N, D1717Q, and D1717K do not bind STX. Besides, the residue at position $i + 1$ can influence toxin block (A1714E). In summary, the structural model we propose is consistent with the toxin sensitivity of the mutants of the SS1-SS2 peptides so far reported.

ENERGETIC IMPLICATIONS OF THE TOXIN BINDING POCKET

Molecular modelling

Modelling was accomplished in the Insight and Discover graphical environments (Biosym Technologies, Inc., San Diego). The molecular mechanics energetic calculations utilized the force field cvff (consistent valence force field), which was specifically derived to fit structures of peptides and proteins. In this approximation the formation of hydrogen bonds is modelled as an electrostatic interaction. For minimization procedures the steepest descents and conjugate gradients have been used.

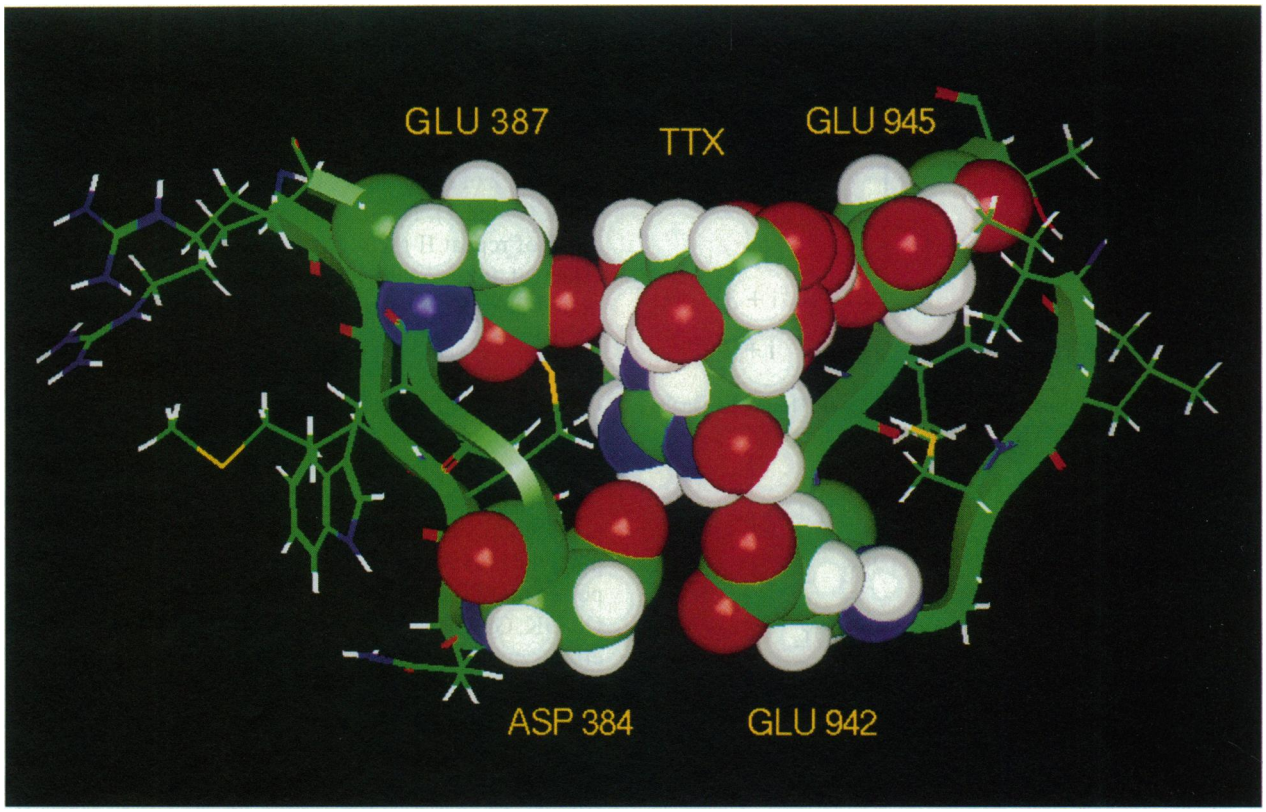

FIGURE 5 Spatial model of the complex of TTX with the beta1 and beta2 strands of repeats I and II of the cardiac Na^+ channel isoform. Four critical carboxyl residues and the TTX are identified as space-filling images, while the remainder of the β-hairpins are shown with a backbone ribbon and stick side chains.

Modelling of the outer vestibule of the Na^+ channel was accomplished in three stages. First, the optimal conformations of the β-hairpins were calculated. Second, the interaction of TTX with the repeat I and II peptides were obtained. The peptides of repeats III and IV were assumed to form only the remaining walls of the pocket. Finally, STX was substituted into the repeat I–II structure derived from interaction with TTX and repeats III and IV were added. The optimal spatial structures of TTX and STX were determined in the same program environment on the basis of their chemical structures and specific configurations (Kao, 1986).

The reasons for modelling the decapeptide of each repeat as a β-hairpin have been discussed, but each residue conformation must be determined. In this structure the two β-strands are united by a β-turn. As zero approximation for angles of rotation $\phi(C^\alpha - N)$ and $\psi(C^\alpha - C')$ in the backbone of the peptide chain of β-strands the angles of rotation in standard antiparallel β-structure, $\phi(C^\alpha - N) = -139°$ and $\psi(C^\alpha - C') = +135°$ (Creighton, 1993) have been taken, while for the two central residues of the β-turns with numbers $i + 1$ and $i + 2$ we used angles of rotation in reverse β-turns of type III: $\phi(C^\alpha - N) = -60°$ and $\psi(C^\alpha - C') = -30°$ (Wilmot and Thornton, 1988). Angles ϕ and ψ in β-strands correspond to region B of conformational maps $\phi - \psi$ ($\phi < 0°$, $\psi > 0°$), while the angles ϕ and ψ in β-turns of type III correspond to region R ($\phi < 0°$, $\psi < 0°$). Therefore we note the corresponding conformational states of the amino acid residues by the symbols B and R.

As a preliminary step during the search for optimal conformation of the β-hairpins of repeats I and II, minimization of potential energy of the pentapeptide fragments on the N and C ends in the conformations BBBBR and RBBBB was carried out. Since only the C ends of the two β-hairpins (the beta2 strands) interact directly with TTX, we found the optimal conformations of repeat I (Asp-Cys-Trp-Glu-Arg (for the cardiac channel), Asp-Tyr-Trp-Glu-Asn (for the muscle channel), and Asp-Phe-Trp-Glu-Asn (for the rat brainII channel)) and of repeat II (Glu-Trp-Ile-Glu-Thr). These pentapeptides were allowed to interact with TTX and new approximations of the angles of rotation $\chi_1(C^\alpha - C^\beta)$, $\chi_2(C^\beta - C^\gamma)$ were obtained for the side chains of residues of Asp and Glu such that they were in maximal proximity to the guanidinium group of TTX. It was possible only when fragments Asp-*X*-*X*-Glu and Glu-*X*-*X*-Glu accepted the conformation RBBB; that is, the conformation of the beta2 strands. After minimization of the energies of these complexes the carboxyl groups of the side chains of Asp and Glu formed optimal hydrogen bonds with the guanidinium group of TTX.

The optimal conformations of the BBBBR fragments of the N ends and the complex conformations derived above for RBBBB of the C ends of the β-hairpins were used to form the two decapeptide β-hairpins of repeats I and II in the

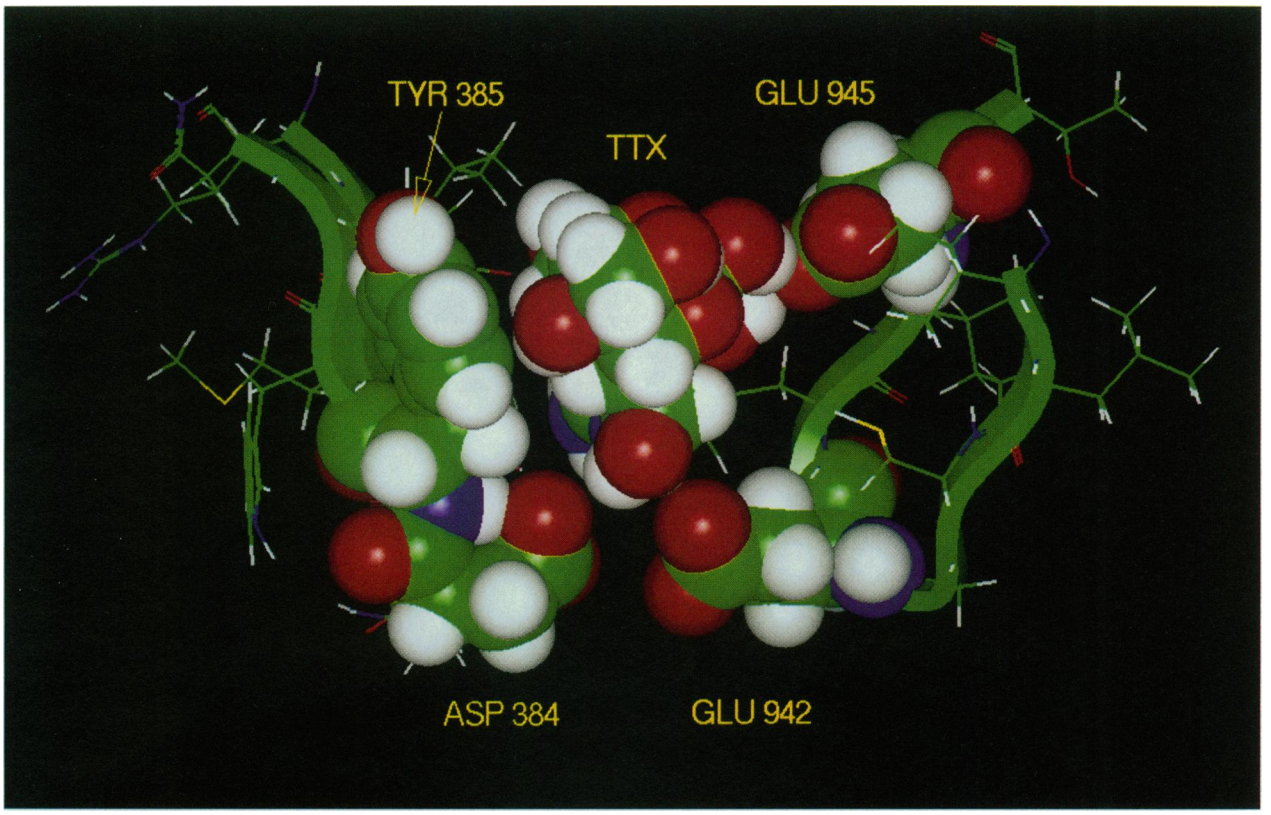

FIGURE 6 Spatial model of the complex of TTX with the beta1 and beta2 strands of repeats I and II of the adult skeletal muscle isoform of the Na^+ channel. The residue Tyr^{385} is also shown in a space-filling image. Note the proximity of the aromatic ring of Tyr to the hydrophobic surface of the TTX.

conformation BBBBRRBBBB. For angles of rotation ϕ and ψ in residues $i + 1$ and $i + 2$ in the β-turns the initial condition that there was a hydrogen bond C═O ··· H—N between residues i and $i + 3$ in the chain was used.

Finally, the three part structure of β-hairpins of repeats I and II and TTX was obtained by combining the TTX molecule in its complexes with the β-hairpins of both repeats I and II for energy minimization of the ensemble. This resulting complex is shown for the cardiac isoform in Fig. 5. The two β-hairpins of repeats I and II form a cavity with the dimensions of TTX. The depth of the cavity is 12–13 Å. The bottom is formed by two carboxyl groups of the side chains of Asp^{384} and Glu^{942} in their $i + 2$ positions on the two β-turns. The distance between the closest oxygens is 4.7 Å, providing room for water molecules in between for compensation of electrostatic repulsion. The distance between the outer carboxyls of Glu^{387} and Glu^{945} are significantly larger at 8.1 Å, so that they could not form direct hydrogen bonds with each other. The back wall of this cavity is formed by the side chain of Trp^{943} of repeat II. As described before, three carboxyls simultaneously form salt bridges with the guanidinium group (Glu^{387} with N(1)—H, Asp^{384} with N(2)—H, and Glu^{942} with N(3)—H), while Glu^{945} forms two optimal hydrogen bonds with the two hydroxyl groups C9-OH and C10-OH of TTX (Fig. 5). The distance between oxygens of the carboxyls and protons of the corresponding N—H groups of TTX in this complex are 2.4–2.6 Å. These distances are slightly greater than the corresponding distances in complexes of TTX with individual chains of repeats I or II (2.1–2.2 Å). In the three part complex the salt bridges have slightly less energy than with only one repeat and TTX. On the other hand, the distances O ··· O in hydrogen bonds formed by side chains of Glu^{945} with C9-OH and C10-OH groups are 3.0 Å, corresponding to optimal hydrogen bonds OH ··· O ((O ··· O) = 2.8 ± 0.1 Å (Pimentel and McClellan, 1960)).

Calculation of the energy of interaction

Nonbonded and electrostatic interactions were calculated. For the complex of repeats I and II and TTX for the cardiac isoform, energies of nonbonded interactions with residues 384, 385, 387, 942, and 945 (rBrII numbering) were −1.5 to −2 kcal/mol, although Trp^{943} had an energy of −4.8 kcal/mol. Electrostatic interactions were calculated using a dielectric constant $\epsilon = 10$, appropriate to calculations for peptide chains in polar (water) media (Krimm and Mark, 1968). Energies of electrostatic interactions for each of the glutamic and aspartic acids, including Glu^{945} with two hydrogen bonds to C9-OH and C10-OH is about −7 kcal/mol. In addition to these, there is electrostatic interaction with the positive side chains of Arg (378, 388, and 937), although there are no nonbonded interactions with them. Therefore, the total of nonbonded and electrostatic interactions of TTX with the β-hairpins of repeats I and II of the cardiac isoform are calculated to be −15.6 and −18.2 kcal/mol, respectively.

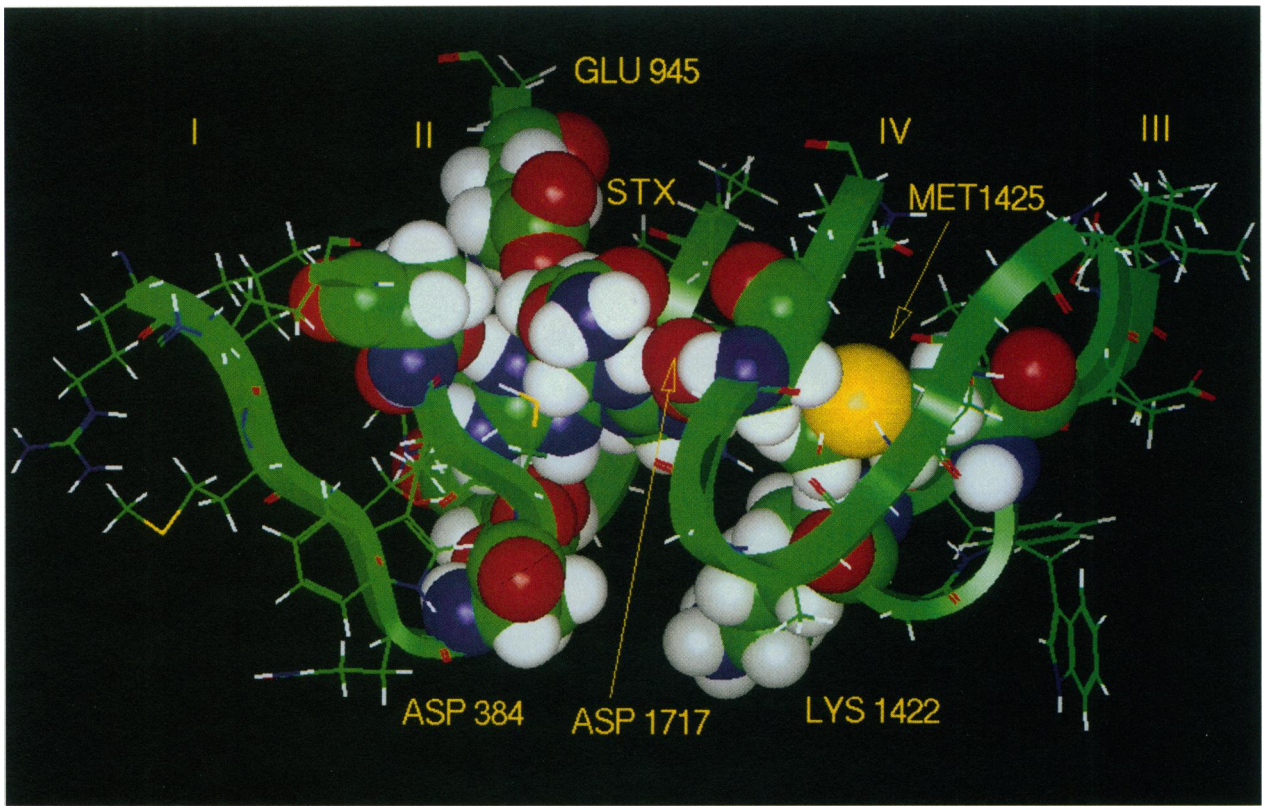

FIGURE 7 Spatial model of the complex of STX with the beta1 and beta2 strands of repeats I–IV of the cardiac Na^+ channel isoform. Note the proximity of the second guanidinium group and carbamyl of STX in the center of the model to Asp^{1717} of repeat IV.

The above calculations were made for the cardiac isoform so that we could compare the model to the experimental results of Satin et al. (1992). They reported that substitution of a Tyr or Phe for Cys^{385} increased the sensitivity of TTX block about 1000 times. This suggests that there is an important nonpolar interaction with TTX. Indeed, TTX has asymmetrical distribution of -OH groups. The surface opposite to the C9 and C10 hydroxyls contains mainly protons of C—H groups. Replacement of the Cys^{385} with either Tyr or Phe causes the aromatic rings to be parallel to the nonpolar surface of TTX (Fig. 6). The nonbonded energy of interaction for tyrosine or phenylalanine is −7 kcal/mol, while that for cysteine is only −2.1 kcal/mol, and energetic gain of about 5 kcal/mol for interaction with the repeat I β-hairpin, as suggested by Satin et al. (1992), and generally supports the structural motif.

The 7,8,9-guanidinium group of STX forms the same physical relationship and energy of interaction as that of the TTX guanidinium group. As before, this group takes part in the same salt bridges with Asp^{384}, Glu^{387}, and Glu^{942}. The interaction of Glu^{945} with two hydroxyls is preserved by the two hydroxyls at C12 of STX. After energy minimization of the three element complex, optimal hydrogen bonds were formed with O ··· O distances of 3.0 A. It is apparent that STX shares the same sites as TTX on repeats I and II, in accordance with the close agreement with their biological action (Kao, 1986). The nonbonded interaction energies are almost identical. However, the second 1,2,3-guanidinium group influences the electrostatic interactions in two ways. The energies of electrostatic interaction of STX with the side chains of Asp and Glu (384, 387, 942, and 945) are larger in absolute scale that those for TTX, but this is compensated by repulsion of the Arg interactions. Consequently, the energies of binding of TTX and STX with the two β-hairpins of repeats I and II are almost identical.

The other two β-hairpins of repeats III and IV were aligned by allowing a salt bridge between the 1,2,3-guanidinium group of STX and the side chain of Asp^{1717} of repeat IV and the presence of van der Waals contacts between STX and the side chain of Met^{1425} of repeat III. Neutralization of Asp^{1717} (D1717N) reduced STX block. Substitution of Gln for Met^{1425} had little effect, but its replacement by the positively charged Lys prevented block (Terlau et al., 1991). We interpret this to mean that the side chain of Met has a nonbonded interaction with STX. Finally, the complex of STX and the four β-hairpins of repeats I–IV was evaluated, including dense packing of β-hairpins but omitting van der Waals repulsions of their neighboring side chains (Fig. 7). In this structure two protons at N(2) of the 1,2,3-guanidinium group form hydrogen bonds with the carboxyl of Asp^{1717}, and the carbamoyl group of STX also takes part in effective electrostatic interactions with this residue of repeat IV. Altogether, the energy of nonbonded and electrostatic interactions of STX with the β-hairpin of repeat IV is −13 kcal/mol. The energy of interaction of STX with the β-hairpin of repeat III is significantly smaller: −1.4 kcal/mol. The Cartesian co-

TABLE 3 Cartesian coordinates (Å) of some groups in the complex of STX with repeats I–IV (World scale system of InsightII)

	Atom	X	Y	Z
Residue				
Repeat I				
Asp^{384}	C^{γ}	16.23	0.86	−5.25
	O	16.09	2.09	−5.40
	O	15.02	0.07	−5.51
Glu^{387}	C^{δ}	12.32	−1.33	−12.01
	O	13.97	−0.79	−12.05
	O	12.10	−1.34	−10.91
Repeat II				
Glu^{942}	C^{δ}	13.10	3.95	−3.11
	O	12.82	2.78	−3.55
	O	14.25	4.42	−3.15
Glu^{945}	C^{δ}	5.52	0.19	−7.22
	O	6.73	0.11	−6.93
	O	4.86	−0.81	−7.57
Repeat III				
Met^{1425}	S^{δ}	11.17	−7.37	0.49
	C^{ϵ}	11.66	−5.64	0.37
	H	11.94	−5.37	−0.66
	H	10.83	−4.98	0.69
	H	12.53	−5.44	1.03
Repeat IV				
Asp^{1717}	C^{γ}	13.61	−8.02	−5.48
	O	13.26	−6.87	−5.24
	O	13.99	−8.47	−6.71
Group of STX				
7,8,9-Guanidinium	N7	11.31	−0.66	−7.70
	H	11.18	−0.49	−8.81
	C8	12.07	0.18	−6.88
	N8	12.78	1.20	−7.33
	H	12.76	1.37	−8.34
	H	13.30	1.75	−6.63
	N9	12.10	−0.19	−5.53
	H	12.56	0.57	−4.81
$C12\text{-}(OH)_2$	C12	9.64	−0.66	−4.76
	O	8.51	−1.51	−5.01
	H	7.83	−0.94	−5.39
	O	9.29	0.64	−5.22
	H	8.65	0.52	−5.93
1,2,3-Guanidinium	N1	11.90	−4.01	−6.06
	H	12.16	−4.99	−6.19
	C2	11.75	−3.58	−4.68
	N2	12.05	−4.48	−3.75
	H	12.37	−5.40	−4.07
	H	11.93	−4.18	−2.77
	N3	11.26	−2.23	−4.35

ordinates of some of the important groups of this complex are given in Table 3.

The difference in energy of interaction between STX and TTX was estimated by substituting TTX for STX in the four β-hairpin model. The nonbonded interaction energies with repeats III and IV are the same, but the loss of the additional electrostatic energy of the 1,2,3-guanidinium group reduced the TTX interaction energy by 6 kcal/mol, giving it a lower affinity than STX. We did not calculate free energy of these interactions, so these values cannot be directly converted into binding affinities for experimental comparison. However, the calculated energy differences between isoforms and between toxins are experimentally consistent.

Although the proposed model of the Na^+ channel vestibule as the toxin binding pocket fits the mutation data presently available, there are several uncertainties to be considered. First, the outside of the pocket faces other parts of the protein, which could have significant effect on the shape and stability of the β-hairpin region. Second, the activities of water and protons in the vestibule could be restricted, affecting the electrostatic interaction energies and the local pH. Finally, the effects of such mutations as K1422E and A1714E (Terlau et al., 1991) do not mean that in native channels Lys and Ala interact with the toxins, because the addition of carboxyls at these sites may create new loci for toxin interaction.

β-TURNS OF THE TOXIN BINDING POCKET FORM THE ION SELECTIVITY FILTER

The mutation studies of Terlau et al. (1991) included estimates of the single channel conductances from noise analysis. Although many of the mutations had no effect on single channel conductance, neutralization of the glutamic acid or aspartic acid residues reduced it. Specifically, neutralization of Asp^{384} (D384N) and Glu^{942} (E942Q) greatly reduced ionic current (Table 1). These residues are located in positions $i + 2$ of β-turns of repeats I and II, and they are apparently involved both in toxin binding and ion conduction of the Na^+ channel. Subsequent studies by Heinemann et al. (1992b) showed that simultaneous mutations of two residues in repeats III and IV (K1422E and A1714E) made the Na^+ channel permeable to Ca^{2+}. They suggested that the resulting four negatively charged side chains at positions 384, 942, 1422, and 1714 reproduce the structure of the selectivity filter of Ca^{2+} channels. Such a change in selectivity is in accordance with our structural model, because the two mutations refer to residues at positions $i + 1$ of the β-turns of repeats III and IV, which because of this antiparallel arrangement are directed to the inside of the binding cavity (Fig. 8). It is interesting to consider the hypothesis that two carboxyls at this site are responsible for Na^+ selectivity of the native Na^+ channel, but that three or four are required for Ca^{2+} permeation.

The ions Na^+ and Ca^{2+} have the same ionic radii (1.02 and 1.00 Å) in crystallohydrates. They are typically octahedrally coordinated with six molecules of water, but because of the difference in charge, they have very different hydration energies (−105 kcal/mole for Na^+ and −397 kcal/mole for Ca^{2+}) (Hille, 1992). This leads to the idea that electrostatic interaction of Na^+ with the two carboxyls at positions 384 and 942 are able to reduce the hydration shell energy sufficient to decrease the barrier to Na^+ movement through the channel pore. However, three carboxyls may be required for weakening of the hydration shell of Ca^{2+}. Three are suggested because the single mutant K1422E and the double mutant K1422E and A1714E have the same Ca^{2+} conductance (Heinemann et al., 1992), so that only the carboxyl at position 1422 may be involved.

In the four β-hairpin model of the Na^+ channel with the toxin removed, Na^+ coordinates with Asp^{384} and Glu^{942} to force out two or more molecules of water. Coordination of

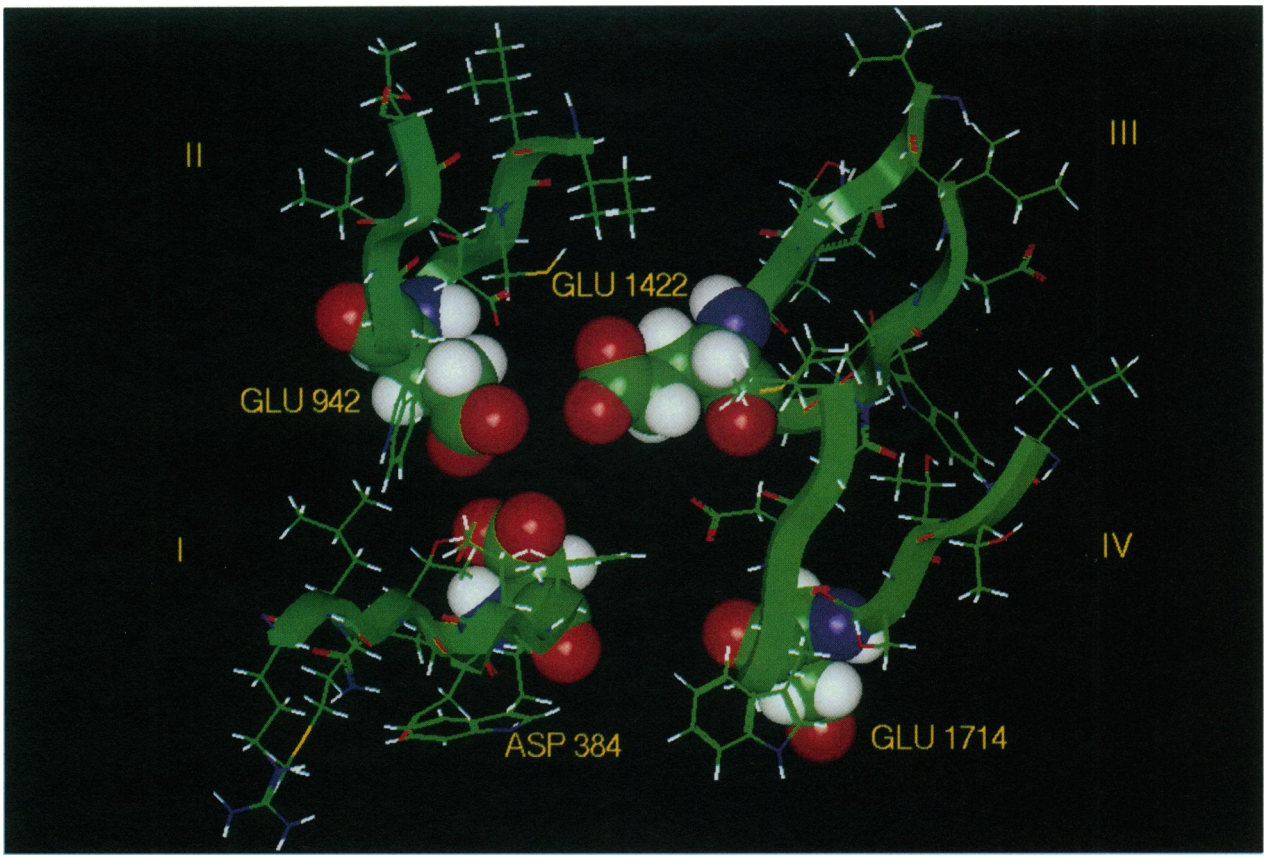

FIGURE 8 Double mutant of the toxin binding site of the Na^+ channel structure with toxin removed (K1422E and A1714E (Heinemann et al., 1992b)).

$Na^+ \cdot 4H_2O$ in this region, which weakens binding energy between Na^+ and water in the transition state is shown in Fig. 9. For the double mutant K1422E and A1714E (Fig. 8), the carboxyls of three side chains (Asp^{384}, Glu^{942}, and Glu^{1422}) can be coordinated with $Ca^{2+} \cdot 3H_2O$, substituting for three molecules of hydration water. In the double mutant model Glu^{1714} does not coordinate with Ca^{2+} because of the asymmetrical structure of this region. This region of the model is similar in size to that suggested by Hille (1971) for the dimensions of the Na^+ channel selectivity filter (3.1 × 5.1 Å). Evidently, selectivity filters in Na^+ and Ca^{2+} channels promote the formation of ions with only one molecule of water ($Na^+ \cdot H_2O$ and $Ca^{2+} \cdot H_2O$), which then pass through the channel pore.

DISCUSSION

The purpose of the model was twofold. Firstly, we wished to determine if the recently available mutation data from cloned Na^+ channels, in combination with the structures of the toxins and their analogs, would lead to a structurally satisfactory toxin binding site. Secondly, defining the site would characterize the structure of part of the permeation path, if the toxin binding site is in the path. Most investigators have assumed that the toxins block by physically occluding the channel, (Hille, 1975; Strichartz, 1984; Kao, 1986). However, Green et al. (1987) have offered biophysical evidence that the toxin binding site is at a distance from the permeation path. The mutation studies of Terlau et al. (1991), Satin et al. (1992), Backx et al. (1992), and Kontis and Goldin (1993) identified several amino acids in the SS1-SS2 regions of each of the four Na^+ channel repeats as critical for toxin binding. Further, Terlau et al. (1991) and Heinemann et al. (1992b) showed that mutations of several of these amino acids change single channel conductance and selectivity of the channel. This demonstration of structural overlap of the toxin binding site and the conductance/selectivity region is strong evidence that the toxin site is indeed in the permeation path.

The proposed model is supported by appropriate interactions with amino acid residues identified by mutation studies and by consistency with the interaction of various toxin analogs. It provides a rationale for differences in binding between TTX, which interacts directly with the SS1-SS2 segments of repeats I and II, and that of STX, which additionally interacts with the segments of repeats III and IV. It also provides a basis for predicting the blocking affinity of new analogs and the effects of other mutations in the binding region. This is illustrated by the model prediction that the differences in toxin binding between the brain/skeletal and the cardiac isoforms is the result of a hydrophobic interaction with the aromatic rings of Phe or Tyr, while Cys may be a spacer element that interacts only weakly.

An unexpected but welcomed outcome of the model was its prediction of the narrow region delineated by residues of

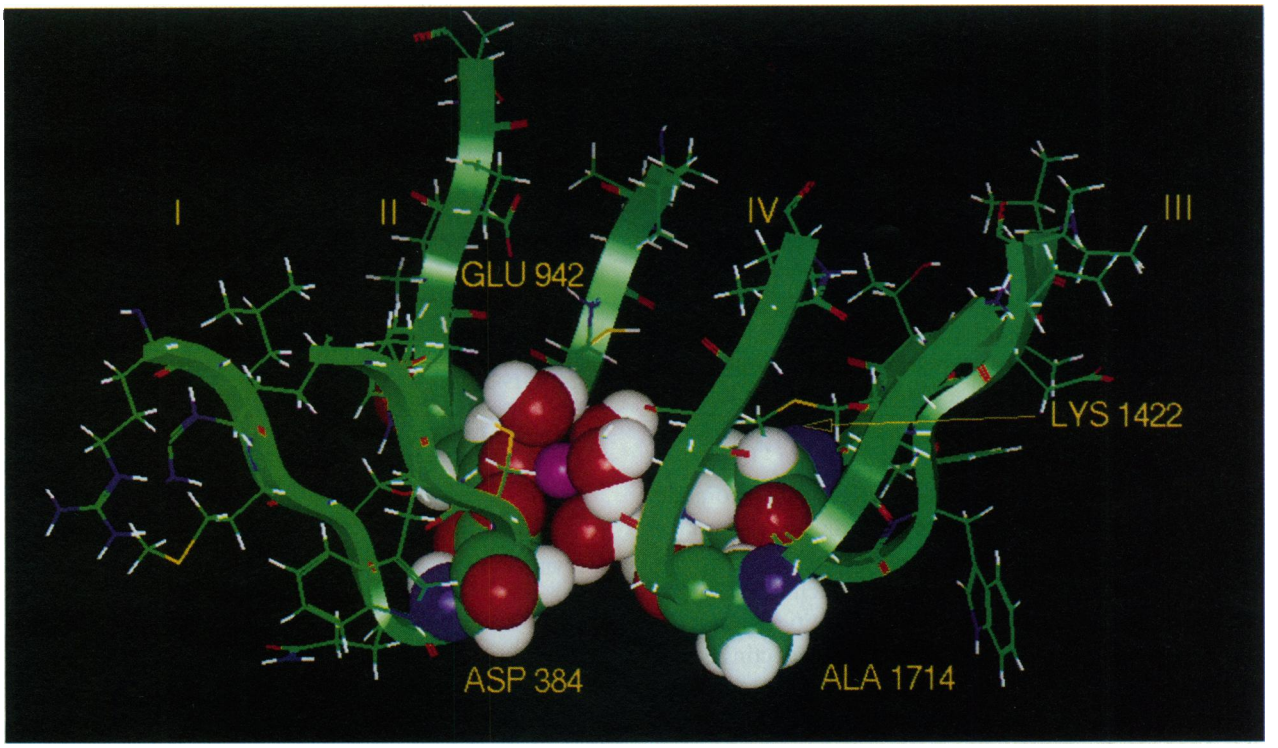

FIGURE 9 Coordination of the hydrated Na^+ ion ($Na^+ \cdot 4H_2O$) with the carboxyls of Asp^{384} and Glu^{942} of the cardiac isoform. Na^+ is in violet. The carboxyls substitute for two of the waters of hydration in the transition state.

the β-turns of the four β-hairpins (384, 942, 1422, 1714). This region has been proposed as a candidate for the selectivity filter by Heinemann et al. (1992b) on the basis of mutation studies. When the toxin was removed from the model pocket formed by the four β-hairpins, the narrow region at the turn points had dimensions close to those predicted by Hille (1971, 1992) on the basis of permeation of organic molecules of various sizes and shapes. Assuming that the molecule is stabilized in this conformation by the rest of the underlying protein, the carboxyl residues at positions 384 and 942 on repeats I and II were located correctly for interaction with the hydrated Na^+ ion ($Na \cdot 6H_2O$), displacing two water molecules and reducing the energy of interaction of the other waters of hydration. However, a third carboxyl on repeat III, shown by Heinemann et al. (1992b) by mutation studies to produce a channel with significant Ca^{2+} permeation, was correctly located in the putative selectivity region to provide an additional displacement of a third water molecule in its hydration shell and decrease the energy of hydration of the other water molecules. We consequently support the suggestion that this region may represent the channel's selectivity filter. Moreover, substitution of either Glu334 or Glu1086 by Lys in the homologous selectivity positions in the human cardiac Ca^{2+} channel α1-subunit leads to a significant increase in Na^+ permeation through the Ca^{2+} channel (Tang et al., 1993). Indeed, according to our model, the spatial arrangement of carboxyls of pairs of glutamic acids 334 and 677 or 677 and 1086, which are necessary for Na^+ permeation of the Ca^{2+} channel is approximately the same as in the triangle of residues 384, 392, and 1422 of the Na^+ channel (Fig. 8).

The appropriate location of the residues of repeat III for simulation of a Ca^{2+} coordination site was the consequence of the antiparallel alignment of the β-hairpins. This does not conflict with possible pseudo 4-fold symmetrical arrangement of the transmembrane segments S1–S6 of repeats I–IV, because the lengths of the segments connecting beta2 to S6 are different. In the case of repeats I and II, they are 9 residues each, whereas for repeats III and IV, they are 19 and 30, respectively, and consequently could accommodate additional loops in repeats III and IV.

Another outcome of the model is the prediction of the structure of the outer vestibule of the channel, defined as the region large enough to accommodate the bulky toxin molecules. The size of this putative vestibule and the location of charged residues are consistent with the modelling studies of Dani (1986) and Cai and Jordan (1990). They provide specific dimensions for future modelling and predictions of the outcomes of mutation studies on surface charge phenomena. This model also allows consideration of interactions between the channel and peptide toxins such as μ-conotoxin, which competes with TTX and STX in blockade of the adult skeletal muscle and eel electroplax channel isoforms (Becker et al., 1992).

In this model the peptide fragments beta1 and beta2 of the P region create only the outer vestibule of the Na^+ channel, with the selectivity filter at its bottom. These peptides do not form the remainder of the transmembrane pore, in contrast

to some previous models of Na^+ and K^+ channels. A simple examination of the P regions shows that the amino acid composition is very different, with many charged residues in the Na^+ channel mouth. Consequently, it is likely that there will be significant differences in the structures of the pore regions of the two channel types.

An important but unresolved question is the possible presence of an electric field in this vestibule and its effect on toxin binding. Schild and Moczydlowski (1991), Satin et al. (1992), Backx et al. (1992), and Doyle et al. (1993) identify a site for divalent ion block within the electric field. Because divalent ion binding is competitive with toxin binding, this implies that there is a field drop within this structural element and predicts that toxin binding should show some voltage dependence.

Although the proposed model is effective in its prediction of isoform/mutation and toxin analog studies, the interface of these four β-hairpins with the rest of the protein could not be considered. It should be clear that such interactions would be important for the shape and stability of the vestibule. The model does provide a basis for selecting other mutations of these peptide segments, which could result in structural refinement, particularly with regard to the mechanism of selectivity.

We thank David Piper for his assistance in the computer simulations, and Dr. Dorothy Hanck for productive discussion during the course of this work. This work was supported in part by PO1-HL20592, the Sprague Memorial Foundation, and the University of Chicago Cardiology Molecular Modelling Core.

REFERENCES

Backx, P., D. Yue, J. Lawrence, E. Marban, and G. Tomaselli. 1992. Molecular localization of an ion-binding site within the pore of mammalian sodium channels. *Science (Wash. DC)*. 257:248–251.

Becker, S., E. Prurak-Sochaczewski, G. Zamboni, A. G. Beck-Sickinger, R. D. Gordon, and R. J. French. 1992. Action of derivatives of μ-conotoxin GIIIA on sodium channels. Single amino acid substitutions in the toxin separately affect association and dissociation rates. *Biochemistry*. 31:8229–8238.

Cai, M., and P. C. Jordan. 1990. How does the vestibule surface charge affect ion conduction and toxin binding in a sodium channel? *Biophys. J.* 57: 883–891.

Catterall, W. A. 1992. Cellular and molecular biology of voltage-gated sodium channels. *Physiol. Rev.* 72:S15-S48.

Chou, P. Y., and G. D. Fasman. 1978. Empirical predictions of protein conformation. *Annu. Rev. Biochem.* 47:251–276.

Creighton, T. E. 1993. Proteins: Structure and Molecular Properties. 2nd ed. W. H. Freeman and Co., New York. 201–269.

Dani, J. A. 1986. Ion-channel entrances influence permeation: net charge, size, shape, and binding considerations. *Biophys. J.* 49:607–618.

Doyle, D., Y. Guo, S. L. Lustig, J. Satin, R. B. Rogart, and H. A. Fozzard. 1993. Divalent cation competition with [^{3}H]saxitoxin binding to tetrodotoxin-resistant and -sensitive sodium channels. *J. Gen. Physiol.* 101:153–182.

Fersht, A. R., J.-P. Shi, J. Knill-Jones, D. M. Lowe, A. J. Wilkinson, D. M. Blow, P. Brick, P. Carter, M. M. Y. Waye, and G. Winter. 1985. Hydrogen bonding and biological specificity analyzed by protein engineering. *Nature (Lond.)*. 314:235–238.

Green, W. N., L. B. Weiss, and O. S. Anderson. 1987. Batrachotoxin-modified sodium channels in planer bilayers. *J. Gen. Physiol.* 89: 873–903.

Guy, H. R., and F. Conti. 1990. Pursuing the structure and function of voltage-gated channels. *Trends Neurol. Sci.* 13:201–206.

Heinemann, S. H., H. Terlau, and K Imoto. 1992a. Molecular basis for pharmacological differences between brain and cardiac sodium channels. *Pflügers Arch.* 422:90–92.

Heinemann, S. H., H. Terlau, W. Stühmer, K. Imoto, and S. Numa. 1992b. Calcium channel characteristics conferred on the sodium channel by single mutations. *Nature (Lond.)*. 356:441–443.

Hille, B. 1968. Pharmacological modifications of the sodium channels of frog nerve. *J. Gen. Physiol.* 51:199–219.

Hille, B. 1971. The permeability of the sodium channel to organic cations in myelinated nerve. *J. Gen. Physiol.* 58:559–619.

Hille, B. 1975. The receptor for tetrodotoxin and saxitoxin: a structural hypothesis. *Biophys. J.* 15:615–619.

Hille, B. 1992. Ionic Channels of Excitable Membranes. 2nd ed. Sinauer Associates, Inc. Sunderland, MA. 59–62.

Kao, C. Y. 1982. Actions of nortetrodotoxin on frog muscle and squid axon. *Toxicon*. 20:1043–1050.

Kao, C. Y. 1986. Structure-activity relations of tetrodotoxin, saxitoxin and analogues. *Ann. N.Y. Acad. Sci.* 479:52–67.

Kao, C. Y., and S. E. Walker. 1982. Active groups of saxitoxin and tetrodotoxin as deduced from action of saxitoxin analogs on frog muscle and squid axon. *J. Physiol. (Lond.)*. 323:619–637.

Kao, C. Y., and T. Yasumoto. 1985. Actions of 4-epitetrodotoxin and anhydrotetrodotoxin. *Toxicon*. 23:725–729.

Kao, C. Y., P. N. Kao, M. R. James-Kracke, F. E. Koehn, C. F. Wichmann, and M. K. Schnoes. 1985. Actions of epimers of 12-(OH)-reduced saxitoxin and of 11-(OSO_3)-saxitoxin on squid axon. *Toxicon*. 23:647–655.

Koehn, F. E., V. E. Ghazarossian, E. J. Schantz, H. K. Schnoes, and F. M. Strong. 1981. Derivatives of saxitoxin. *Bioorg. Chem.* 10:412–428.

Kontis, K. J., and A. L. Goldin. 1993. Site-directed mutagenesis of the putative pore region of the rat IIA sodium channel. *Mol. Pharmacol.* 43:635–644.

Krimm, S., and J. Mark. 1968. Conformations of polypeptides with ionized side chains of equal length. *Proc. Natl. Acad. Sci. USA*. 60:1122–1129.

Mahar, J., G. L. Lucacs, Y. Li, S. Hall, and E. Moczydlowski. 1991. Pharmacological and biochemical properties of saxiphilin, a soluble saxitoxin-binding protein from the bullfrog. *Toxicon*. 29:53–71.

Narahashi, T., J. W. Moore, and R. N. Posten. 1967. Tetrodotoxin derivatives. Chemical structure and blockage of nerve membrane conductance. *Science (Wash. DC)*. 156:976–979.

Narahashi, T. 1974. Chemicals as tools in the study of excitable membranes. *Physiol. Rev.* 54:813–889.

Noda, M., S. Shimazu, T. Tanabe, T. Takai, T. Kayano, T. Ikeda, M. Takahashi, H. Nakayama, Y. Kanaoka, N. Minamino, et al. 1984. Primary structure of *Electrophorus electricus* sodium channel deduced from cDNA sequence. *Nature (Lond.)*. 312:121–127.

Noda, M., H. Suzuki, S. Numa, and W. Stühmer. 1989. A single point mutation confers tetrodotoxin and saxitoxin insensitivity on the sodium channel-II. *FEBS Lett.* 259:213–216.

Numa, S., and M. Noda. 1986. Molecular structure of sodium channels. *Ann. N.Y. Acad. Sci.* 479:338–355.

Pimentel, G. C., and A. L. McClellan. 1960. The Hydrogen Bond. Freeman Sc. Co., London. 265–285.

Proegman, J. H., G. Drent, K. H. Kalk, and W. G. T. Hol. 1978. Structure of bovine liver rhodanese. *J. Mol. Biol.* 123:557–594.

Satin, J., J. W. Kyle, M. Chen, P. Bell, L. L. Cribbs, H. A. Fozzard, and R. B. Rogart. 1992. A mutant of TTX-resistant cardiac sodium channels with TTX-sensitive properties. *Science (Wash. DC)*. 256:1202–1205.

Schild, L., and E. Moczydlowski. 1991. Competitive binding interaction between Zn^{2+} and saxitoxin in cardiac Na-channels. *Biophys. J.* 59: 523–537.

Schrager, P., and C. Profera. 1973. Inhibition of the receptor for tetrodotoxin in nerve membranes by various modifying carbonyl groups. *Biochim. Biophys. Acta*. 318:141–146.

Sibanda, B. L., T. L. Blundell, and J. M. Thornton. 1989. Conformations of β-hairpins in protein structures. *J. Mol. Biol.* 206:759–777.

Strichartz, G. 1984. Structural determinants of the affinity of saxitoxin for neuronal sodium channels. *J. Gen. Physiol.* 84:281–305.

Tang, S., G. Mikala, A. Bahinski, A. Yatani, G. Varadi, and A. Schwartz.

1993. Molecular localization of ion selectivity sites within the pore of a human L-type cardiac calcium channel. *J. Biol. Chem.* 268:13026–13029.

Terlau, H., S. H. Heinemann, W. Stühmer, M. Pusch, F. Conti, K. Imoto, and S. Numa. 1991. Mapping the site of block by tetrodotoxin and saxitoxin on sodium channel–II. *FEBS Lett.* 293:93–96.

Tomaselli, G. F., H. B. Nuss, J. H. Lawrence, P. H. Backx, and E. Marban. 1993. A cysteine substitution in the P-region of the skeletal muscle sodium channel alters sensitivity to tetrodotoxin and divalent cations. *Biophys. J.* 64:A88. (Abstr.)

Williams, R. W., A. Chang, D. Juretic, and S. Longhran. 1987. Secondary structural predictions and medium range interactions. *Biochim. Biophys. Acta.* 916:200–204.

Wilmot, C. M., and J. M. Thornton. 1988. Analysis of different types of β-turns in proteins. *J. Mol. Biol.* 203:221–232.

Yang, L., and C. Y. Kao. 1992. Actions of chiriquitoxin on frog skeletal muscle fibers and implications for the tetrodotoxin/saxitoxin receptor. *J. Gen. Physiol.* 100:609–622.

Yang, L., C. Y. Kao., and T. Yasumoto. 1992a. Actions of 6-epitetrodotoxin and 11-deoxytetrodotoxin on the frog skeletal muscle fiber. *Toxicon.* 30: 635–643.

Yang, L., C. Y. Kao, and Y. Oshima. 1992b. Actions of decarbamoyloxysaxitoxin and decarbamoylneosaxitoxin on the frog skeletal muscle fiber. *Toxicon.* 30:645–652.